2006

Bowtie Compressor With Novel Capacity Modulation Part 2: Model Validation and Parametric Studies

Junhyeung Kim
Purdue University

Eckhard A. Groll
Purdue University

Bowtie Compressor with Novel Capacity Modulation Part 2: Model Validation and Parametric Studies

Jun-Hyeung Kim*, Eckhard A. Groll

Purdue University,
School of Mechanical Engineering,
Ray W. Herrick Laboratories
West Lafayette, IN. 47907, USA

*Corresponding Author: phiengineer@gmail.com

ABSTRACT

A novel refrigeration compressor with an integrated method of capacity modulation for use in domestic refrigerators/freezers is proposed and analyzed here. The compressor is called bowtie compressor due to its two sector-shaped, opposing compression chambers forming a bowtie. The bowtie compressor modulates the cooling capacity by changing the piston stroke without changes of the clearance volume for better thermodynamic efficiency. The new compressor includes a unique off-center-line mechanism so that the piston stroke can be varied without changes in motor rotation. To investigate the feasibility of the proposed compressor, a simulation model has been developed. The validation of the simulation methodology and parametric studies to see how the proposed compressor performance can be improved are presented in this Part II paper.

1 INTRODUCTION

In Part I of the paper (Kim and Groll, 2006), a bowtie compressor with novel capacity modulation was described in detail. In addition, a simulation model that predicts the performance of the bowtie compressor was presented. This Part II paper discusses the model validation, the simulation results, and parametric studies.

2 VALIDATION OF THE SIMULATION METHODOLOGY

The best way to validate a simulation model is to compare the model results with actual calorimeter test data of a prototype compressor. However, without the support of a compressor manufacturing company, it is technically difficult to build a prototype and test it. Since the proposed bowtie compressor is a new compressor type, there are also no test data available in the literature. Thus, an indirect method is employed to validate the simulation model. The model was modified to predict the thermodynamic performance of a reciprocating compressor, and the predictions are compared to available test data for this compressor. Once the modified model is validated, then the original model will be regarded as sufficiently validated to predict the performance of the bowtie compressor. This is based on the fact that a bowtie compressor can be closely modeled as a reciprocating compressor due to its reciprocating piston motion

The bowtie compressor simulation model was modified to simulate a reciprocating compressor, which uses R-134a as the refrigerant and is designed for low back pressure applications with a cooling capacity of 267 W at the operating conditions of T_{cond}=54.4˚C, T_{evap}=-23.3˚C, and T_{amb}=T_{suct}= 32.2˚C for domestic refrigerators/freezers. Modifications were made with respect to the analysis of the kinematics, the analysis of the dynamics, the friction loss model and the overall compressor analysis. The modifications were done where different structures were found. Then, the reciprocating compressor model is directly compared to the calorimeter data and to the compressor map obtained from the manufacturer.

2.1 Comparison to the Calorimeter data

Table 1 presents the basic geometric parameters of the reciprocating compressor. The reciprocating compressor is simulated at the following conditions: condensing temperature of 54.4˚C, evaporating temperature of -23.3˚C, and suction and ambient temperatures of 32.2˚C. Since the clearance volume and the piston clearance to the cylinder

wall of the reciprocating compressor are not known, the simulation model is tuned based on a comparison of the calorimetric and the simulated results by adjusting the fraction of the hot gas back-flow in the shell as discussed by Meyer (1987) and the clearance between piston and cylinder wall.

Table 1: Reciprocating geometric parameters.

Cylinder Diameter	22.44 mm	Crank Radius	9.1 mm
Piston Clearance	Not Known	Connecting Rod Length	40.4 mm
Suction Port Diameter	8.0 mm	Discharge Port Diameter	3.5 mm

The effect of a fraction of the hot gas back-flow, α, on the cylinder inlet temperature and the compressor mass flow rate is shown in Figure 1. The figure shows that the cylinder inlet temperature increases linearly with the fraction of the hot gas back-flow. This is because more hot gas in the compressor shell is mixed with the suction gas. On the other hand, the compressor mass flow rate decreases with the fraction of the hot gas back-flow. This is due to the fact that as the cylinder inlet temperature increases, the refrigerant density decreases. To closely match the cylinder inlet temperature of the simulation with the one of the calorimeter data, which is 61.6˚C, a fraction of the hot gas back-flow was set at 0.47.

Figure 2 shows the effect of the piston clearance on the mass flow rate when a fraction of the hot gas back-flow is fixed as 0.47. A decrease of the piston clearance results in more mass flow rate, approximately 9 % when the piston clearance is changed from 10 μm to 5 μm. At a piston clearance of 5 μm, the simulated mass flow rate of 1.42 g/sec is very close to the actual mass flow rate of 1.43 g/sec. The difference is approximately 1 %. Different piston clearances do not have much impact on the cylinder inlet temperature as shown in Figure 2. The cylinder inlet temperature stays relatively close to the actual cylinder inlet temperature of 61.6˚C.

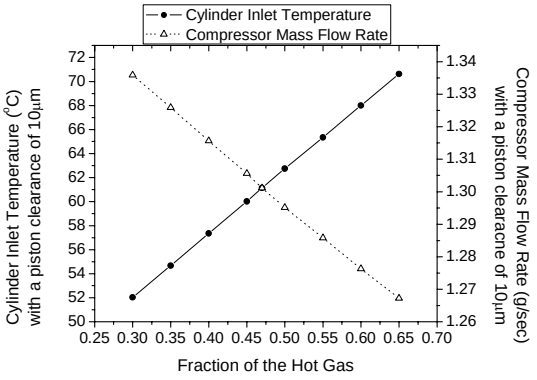

Figure 1: Effect of a fraction of the hot gas.

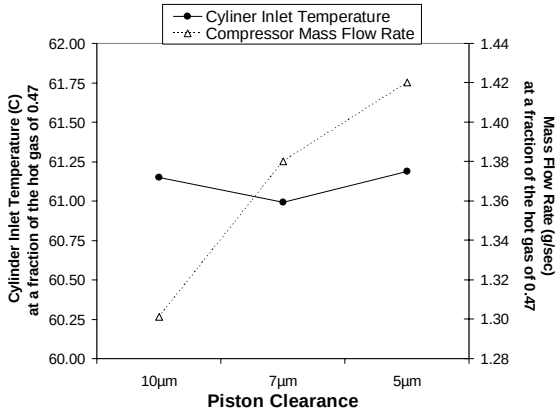

Figure 2: Effect of different piston clearances.

Based on these comparative analyses, the reciprocating compressor model is tuned by setting the fraction of the hot gas back-flow to 0.47 and the piston clearance to 5 μm. This results in very close predictions of the cylinder inlet temperature, the compressor mass flow rate, the power consumption, and the EER from the calorimeter data. Table 2 shows a comparison of the results of the tuned reciprocating compressor model to the calorimeter data. It has to be noted that a big difference exists at the discharge temperature. One explanation is that the current heat transfer models are not adequate when using a forced convective heat transfer coefficient at the discharge cavity and a free convective heat transfer coefficient at the discharge line. Another explanation is that the temperature measurement at the discharge may have been faulty since the temperature difference is too large to predict by using the heat transfer coefficients logically applied at the discharge cavity and the discharge line. Considering that the tuned reciprocating compressor model predicts the other points very well, it seems that the second explanation is more likely, but no proof can be supplied to back up this claim.

Detailed calorimeter data of the reciprocating compressor are only available at one operating conditions. Thus, the simulation results are compared to the manufacturer's compressor performance map. Figures 3, 4, and5 show comparisons of the predicted and the listed mass flow rates, power consumptions, and EER, respectively. The comparison results reveal that the simulation model predicts the mass flow rate within 7 %, the power consumption within 1 %, and the EER within 8 %. It is noticed that the model predicts the mass flow rate and the EER more

accurately at the evaporating temperature of -23.3˚C than at the other evaporating temperatures. This is due to the fact that the model was tuned at the evaporating temperature of -23.3˚C. The differences between the mass flow rate and the EER tend to increase with evaporating temperature but are still within 8 % throughout.

Table 2: Comparison of the calorimeter data to the simulated results.

Piston Clearance: 5μm; Fraction of the Hot Gas:0.47					
Mass Flow Rate (g/sec)			Cylinder Inlet Temperature (C)		
Calorimeter	Simulation	Difference(%)	Calorimeter	Simulation	Difference(K)
1.434	1.420	-0.95	61.6	61.19	0.41
Cylinder Outlet Temperature (C)			Discharge Temperature (C)		
Calorimeter	Simulation	Difference(K)	Calorimeter	Simulation	Difference(K)
124.4	125.91	1.51	72.1	110.59	38.49
Power Input (W)			EER		
Calorimeter	Simulation	Difference(%)	Calorimeter	Simulation	Difference(%)
170	171.19	0.7	5.353	5.252	-1.9

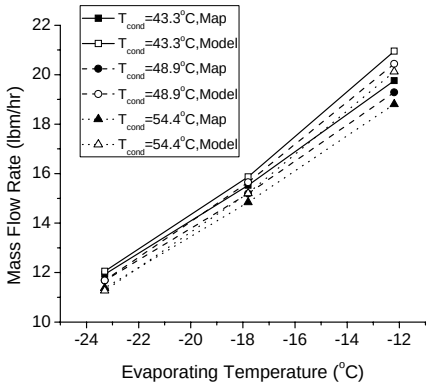

Figure 3: Comparison of the mass flow rate between the compressor map and the model.

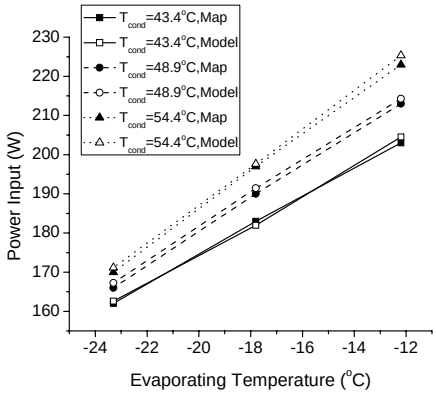

Figure 4: Comparison of the power input between the compressor map and the model.

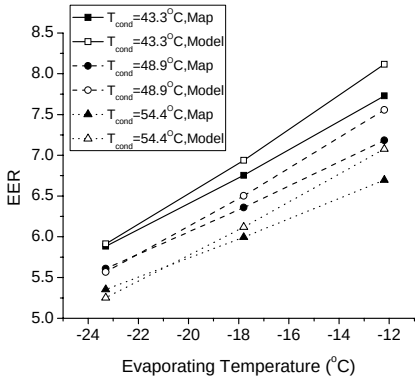

Figure 5: Comparison of the EER between the compressor map and the model.

The comparisons of the simulation results to the calorimeter data and the compressor map shows that the simulation methodology of the reciprocating compressor model is appropriate. Since the bowtie compressor model is similar to the reciprocating compressor model in many ways, the bowtie compressor model is assumed to be validated in order to conduct the theoretical bowtie compressor performance analysis.

3 SIMULATION MODEL RESULTS

The bowtie compressor is simulated using R-134a as the refrigerant at the operating conditions of T_{cond}=54.4˚C, T_{evap}=-23.3˚C, and T_{amb}=T_{suct}= 32.2˚C. While the compressor swept volume is varied from 3.04 cm^3 to 4.70 cm^3 in each chamber, the clearance volume for each camber is fixed at 0.12 cm^3. All leakage clearances are set to 2.5 μm. Table 1 lists the geometric parameters of the bowtie compressor that are used in the simulation unless indicated otherwise.

Table 2: Bowtie compressor geometric parameters.

Vane Height	15 mm	Vane Radius	35 mm
Vane Thickness	4.4 mm	Cylinder Journal Bearing Radius	10 mm
Connecting Rod Length	80 mm	Eccentricity Rod	10 mm
Suction Port Diameter	8.0 mm	Discharge Port Diameter	4.5 mm
Leakage Clearances	2.5μm		

3.1 Effect of changes on the swept volume

Figure 6 shows how the pressure-volume diagrams changes with five swept volumes. The swept volume increases by approximately 55% from 3.04 cm^3 to 4.70 cm^3. This can be achieved by increasing the control length, x, from the reference point, where the minimum swept volume occurs, to 2.0 cm. The proposed compressor will always start up with the minimum swept volume because the cylinder module is spring biased. Thus, at default, the cylinder module is positioned at x = 0 cm. While the clearance volume stays unchanged, the swept volume increases with the control distance. Consequently, the compressor work, the enclosed area of a Pressure-Volume diagram, increases. The figure also shows that the over-compression during the discharge process gradually decreases as the swept volume decreases. This is mainly because a decrease in swept volume results in a lower refrigerant mass flow rate, which in turn creates less flow restriction through the same discharge port. It is difficult to see from the figure, but the expansion volume also decreases when the swept volume decreases. This is due to the reduced remnant refrigerant in the same clearance volume, which requires the compressor to have less expansion volume.

The predictions of the volumetric, the clearance volume and the motor efficiencies are plotted in Figure 7. Two important predictions have to be pointed out. First, the volumetric and the clearance volume efficiencies decrease with swept volume. The main reason for this behavior is that the volume during the suction process and the refrigerant volumetric flow rate at the cylinder inlet decrease as the swept volume decreases. However, it should be noted that since the clearance volume stays constant and less expansion volume is required, the bowtie compressor should have a lower rate of decreases in volumetric and clearance volume efficiencies than typical variable stroke compressors. It should also be noted that the clearance volume efficiency is different from the volumetric efficiency. The clearance volume efficiency does not consider the gas density at the cylinder inlet. Second, the motor efficiency decreases from 83 % to 76.2 %. This shows that for the given capacity modulation mode, the current motor of the bowtie compressor moves away from the plateau of the motor map, where changes in the motor efficiency are very small.

Figure 8 presents the prediction of the compressor mass flow rate and the overall isentropic compressor efficiency as a function of the swept volume. At these operating conditions, the model of the bowtie compressor predicts a 52 % reduction in compressor mass flow rate from 1.504 g/sec to 0.722 g/sec with an approximately 21 % decrease in overall isentropic compressor efficiency from 59.65 % to 47.38 %. One reason for the decrease in overall isentropic compressor efficiency is that the motor runs off its optimum efficiency at the low capacity conditions. This is not unexpected given that fixed motors are optimized for a certain range where the maximum cooling capacity can be achieved. The compressor mass flow rate decreases almost linearly with the swept volume. This indicates that a linear controller as the actuator can be used to achieve continuous capacity modulation.

The frictional power loss and the mechanical efficiency are presented in Figure 9. The frictional power loss and the mechanical efficiency decrease approximately 22 % from 17.2 W to 13.5 W and approximately 5 % from 89 % to 84.6 %, respectively. It is observed that both of the frictional power loss and the mechanical efficiency decrease with a reduction in swept volume. When the swept volume decreases, the swept area where friction occurs reduces, which causes less frictional power loss. However, at the same time, the compressor shaft power decreases as well. This explains that the mechanical efficiency decreases even though the frictional power loss decreases.

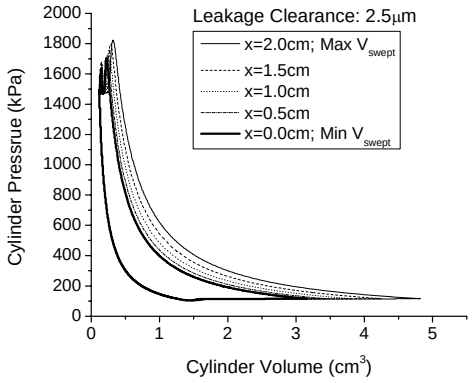

Figure 6: Compression cycles on the Pressure and Volume diagram.

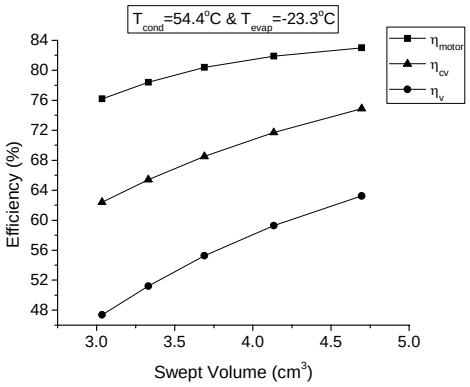

Figure7: Effect of swept volume on volumetric, clearance volume, and motor efficiencies.

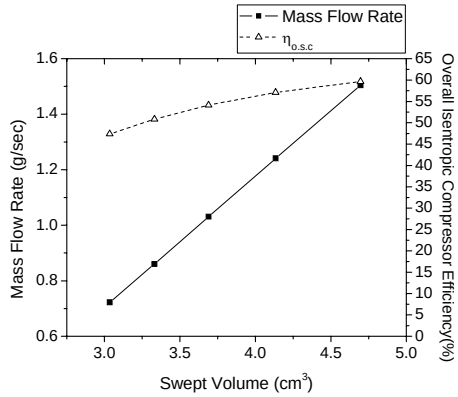

Figure 8: Effect of swept volume on mass flow rate and overall isentropic compressor efficiency.

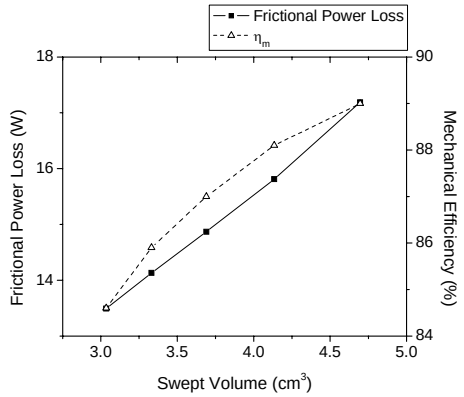

Figure 9: Effect of swept volume on frictional power loss and mechanical efficiency.

3.2Effect of changes of the clearances of the leakage passages

The bowtie compressor is simulated with the same geometric parameters listed in Table 2 except that the leakage clearances are varied from 0.5 to 5.0 μm.

Figure 10 shows the fractional leakage flow rate, which is defined as a ratio of average leakage flow rate to actual compressor flow rate. The fractional leakage flow rates through the five leakage flow paths are stacked up for each case of leakage clearance. The total fractional leakage flow rate decreases from 36 % to 0.6 % when the clearance is reduced from 5.0 μm to 0.5 μm. The results show that the largest leakage occurs in Leak02, i.e., leakage over the vane. It comprises approximately 73 % of the total leakage flow for each case of leakage clearance.

The frictional loss and the compressor mass flow rate as a function of leakage clearance are shown in Figure 11. The figure indicates that the mass flow rate starts to increase and then flattens out at a clearance of 1.0 μm when the leakage clearance is varied from 5.0 to 0.5 μm. Meanwhile, the frictional loss slowly increases and then shoots up dramatically at a clearance of 1.5 μm when the leakage clearance is varied from 5.0 to 0.5μm. These trends strongly indicate that the performance gain due to an increase in mass flow rate with smaller clearances at some point reverses to a performance loss due to the increase in frictional losses. The increase in frictional losses implies that the viscous shear stress in the leakage path is more sensitive to changes in the Couette flow than in the Poisson flow.

Figure 12 presents the clearance volume and the volumetric efficiencies as a function of leakage clearance. The figure indicates that the clearance volume efficiency and volumetric efficiency have opposite trends when the leakage clearance increases. The clearance volume efficiency increases by 7.2 % to a value of 78.5 % whereas the volumetric efficiency decreases approximately 20.6 % to a value of 53.5 % as the leakage clearance increases from 0.5 to 5.0 μm. The reason for the decreasing volumetric efficiency is that the mass flow rate decreases. The

increasing trend in the clearance volume can be explained by considering trapped refrigerant mass in the clearance volume. As the clearance increases, less amount of refrigerant is trapped in the clearance volume due to the increased leakage. As a result, the expansion volume decreases. Thus, the clearance volume efficiency increases since the clearance volume and swept volume are kept the same.

Figure 13 shows the overall isentropic efficiency as a function of leakage clearance. The figure shows that there is an optimum leakage clearance where the best compressor performance can be achieved. The figure indicates that in a clearance range of 1.0 and 5.0 μm, the compressor tends to perform better with smaller clearance because the performance gain of the increased mass flow rate offsets the performance loss due to the increased frictional loss. The overall isentropic compressor efficiency is improved by approximately 22 % when the leakage clearance is decreased from 5.0 μm to 1.0 μm. However, as the leakage clearance is further reduced to 0.5 μm, the overall isentropic efficiency decreases because the performance loss due to the increased frictional loss is larger the gain of the increased flow rate.

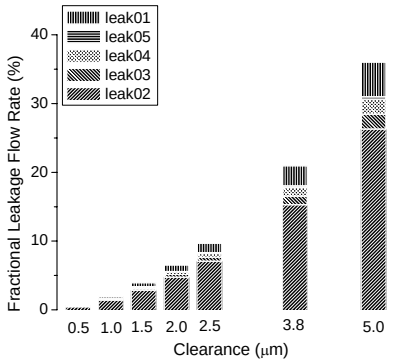

Figure 10: Effect of clearance on leakage.

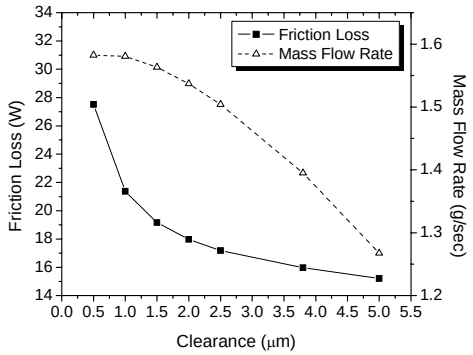

Figure 11: Effect of clearance on friction loss and mass flow rate.

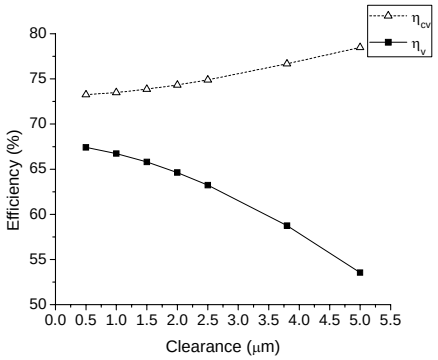

Figure 12: Effect of clearance on volumetric and clearance volume efficiencies.

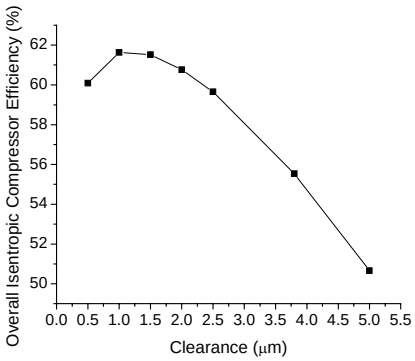

Figure 13: Effect of clearance on overall isentropic compressor efficiency.

Table 3: Ratio of the vane radius to the vane height.

Swept Volume = 4.696cm^3, Swept Angle = 30.05˚ Clearance Volume = 0.12cm^3, Leakage Clearance = 2.5μm									
Ratio	0.5	0.75	1	1.25	1.5	1.75	2	2.25	2.5
Vane Radius (mm)	21.99	24.73	26.95	28.84	30.5	31.99	33.35	34.6	35.77
Vane Height (mm)	43.98	32.98	26.95	23.07	20.33	18.28	16.67	15.38	14.31
Swept Volume = 4.696cm^3, Swept Angle = 25.05˚ Clearance Volume = 0.12cm^3, Leakage Clearance = 2.5μm									
Ratio	0.5	0.75	1	1.25	1.5	1.75	2	2.25	2.5
Vane Radius (mm)	23.57	26.57	28.99	31.05	32.86	34.49	35.97	37.34	38.61
Vane Height (mm)	47.14	35.43	28.99	24.84	21.91	19.71	17.99	16.59	15.44

3.3 Effect of a ratio of the vane radius to the height

The bowtie compressor is simulated by using ratios of the vane radius to the vane height as shown in Table 3 while maintaining the same swept volume and angle.

Figure 14 presents that the mass flow rate and the overall isentropic efficiency at two different swept angles as a function of the ratio of the vane radius to the vane height. The figure shows that in each case of swept angle the compressor mass flow rate and the overall isentropic efficiency have maximum values at the same ratio of 1.25. In each case of swept angle, it is observed that the minimum leakage occurs at the ratio of 1.25. This explains why the maximum compressor mass flow rate is achieved at that ratio.

Consequently, the results show that there is an optimum combination of the vane radius and vane height to achieve the maximum compressor performance at fixed leakage clearance and swept volume. It is shown that the optimum ratio does not change with swept angles.

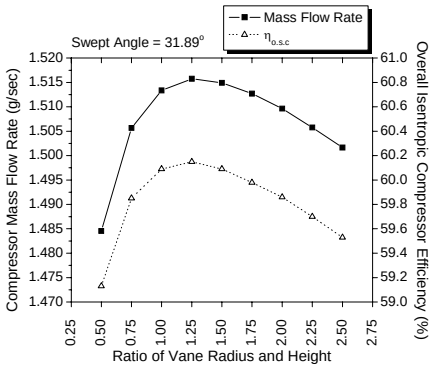

(a) At the swept angle of 31.89˚.

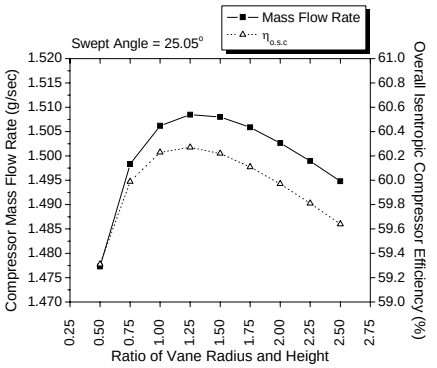

(b) At the swept angle of 25.05˚.

Figure 14: Effect of a ratio of the vane radius and height on compressor mass flow rate and overall isentropic compressor efficiency.

3.4 Study of the compressor performance with optimum parameters

It was shown that the compressor performance could be increased either by using the optimum ratio of vane radius to vane height or by using the optimum leakage clearance. This finding strongly suggests that there is a combination of these two parameters at which the compressor has an optimum performance.

Figure 15 presents how much the overall isentropic efficiency improves by using both the optimum ratio of vane radius to vane height and the optimum leakage clearance. The first case was simulated with a swept volume of 4.696 cm^3, a leakage clearance of 2.5 μm, and a ratio of vane radius to vane height of 2.33. In the second case, the optimum ratio of vane radius to vane height, 1.25, was used while the other parameters stayed the same. In the third case, the leakage clearance was changed from 2.5 to 1.0 μm in addition to using the optimum ratio of vane radius to vane height. Figure 15 shows that the change of the ratio of vane radius to vane height improves the overall isentropic efficiency by approximately 1 % to a value of 60.1 %, and that the changes of both the ratio and the leakage clearance improves the overall isentropic efficiency by approximately 4 % to a value of 62 %.

4 CONCLUSIONS

A novel method of capacity modulation of refrigeration compressors as used in domestic refrigerators/freezers is proposed. The new method modulates the cooling capacity by changing the piston stroke without changes of the clearance volume for better thermodynamic efficiency. The new method is implementing a unique off-center-line mechanism so that the piston stroke can be varied without changes in motor rotation. Due to its geometric shape, the new compressor is called bowtie compressor.

A complete simulation model of the bowtie compressor was developed and validated. Furthermore, parametric studies were carried out to investigate the effects of using different geometric parameters on compressor performance. The effects of leakage clearances and the ratio of the vane radius to the vane height while keeping the swept volume constant on compressor performance were studied. The result showed that the bowtie compressor is able to control its mass flow rate (and thus, its cooling capacity) from 50 to 100 % using an electronic control valve.

Since the proposed compressor has more leakage paths than conventional reciprocating compressors, the effect of changes of the leakage clearances was studied. The simulation results showed that the compressor performance improved as the leakage clearances decreased from 5.0 to 1.0 μm. The reduction in leakage clearance adversely increased the friction loss and decreased the mechanical efficiency, but the overall isentropic compressor efficiency improved because the reduced leakage flow rate increased the mass flow rate of the compressor. However, as the leakage clearance is further reduced to 0.5μm, the compressor performance decreased. At that point, the increased mass flow rate could not compensate the performance loss by the increased frictional loss. Even though the model predicted that the maximum compressor performance would occur at the clearance of 1.0μm, it has to be noted that reducing the clearance to 1.0 μm may not be practical due to manufacturing costs and challenges. Instead, it would be more feasible to increase the vane thickness so that the maximum compressor performance occurs at larger leakage clearance than 1.0μm.

The study of using different ratios of the vane radius to the vane height while maintaining the same swept volume demonstrated that there is an optimum ratio of vane radius to vane height to achieve the maximum compressor performance at a given swept volume. The optimum ratio of the studied bowtie compressor with the swept volume of 4.7cm^3 is found to be 1.25 and does not change with different swept angles.

Although the presented results are solely based on theoretical models and need to be verified using experimental data, it is reasonable to believe that these results capture trends of the actual bowtie compressor performance. The current simulation model can be used as a tool to prototype a bowtie compressor.

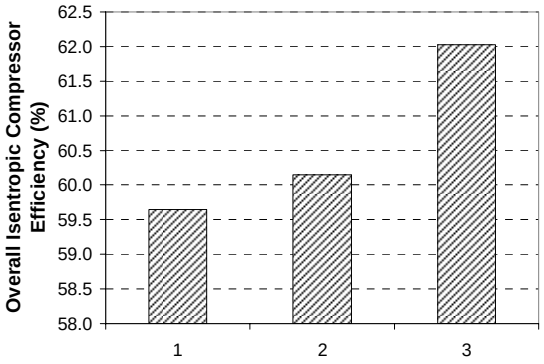

Case 1: leakage clearance of 2.5μm and a ratio of the vane radius to the vane height of 2.33.

Case 2: leakage clearance of 2.5 μm and the optimum ratio of vane radius to vane height of 1.25.

Case 3: leakage clearance of 1.0 μm and the optimum ratio of vane radius to vane height of 1.25.

Figure 15: Overall isentropic compressor efficiency in three representative cases.

NOMENCLATURE

EER	energy efficiency ratio (Btu hr^{-1} W^{-1})
T_{amb}	ambient temperature (C)
T_{cond}	condensing temperature (C)
T_{evap}	evaporating temperature (C)
T_{suct}	compressor suction temperature(C)
V_{swept}	compressor swept volume (m^{-3})
x	control length (cm)

Greek letters

η_{cv}	clearance volume efficiency
η_m	mechanical efficiency
η_{motor}	motor efficiency
$\eta_{o,s,c}$	overall isentropic compressor efficiency
η_v	volumetric efficiency

REFERENCES

Kim, J.-H, Groll, E. A., 2006, Bowtie compressor with novel capacity modulation, Part I: Design description and model development, *Proceedings of International Compressor Engineering Conference at Purdue*, C150.

Meyer, W. A., 1987, *An Investigation into Heat Transfer Processes in a Small Hermetic Refrigeration Compressors*, MSME Thesis, Purdue University, West Lafayette, IN.